Langmuir probe measurements of the electron energy distribution function in magnetized gas discharge plasmas

2012 Plasma Sources Sci. Technol. 21 025004

(http://iopscience.iop.org/0963-0252/21/2/025004)

Plasma Sources Sci. Technol. **21** (2012) 025004 (10pp) doi:10.1088/0963-0252/21/2/025004

Langmuir probe measurements of the electron energy distribution function in magnetized gas discharge plasmas

Tsv K Popov[1], P Ivanova[2], M Dimitrova[2], J Kovačič[3,6], T Gyergyek[3,4,6] and M Čerček[4,5,6]

[1] Faculty of Physics, St. Kl. Ohridski University of Sofia, 5, J. Bourchier Blvd., 1164 Sofia, Bulgaria
[2] Emil Djakov Institute of Electronics, Bulgarian Academy of Sciences, 72, Tzarigradsko Chaussee, 1784 Sofia, Bulgaria
[3] University of Ljubljana, Faculty of Electrical Engineering, Tržaška 25, 1000 Ljubljana, Slovenia
[4] Jožef Stefan Institute, Jamova 39, 1000 Ljubljana, Slovenia
[5] University of Maribor, Faculty of Civil Engineering, Smetanova 17, 2000 Maribor, Slovenia
[6] Association EURATOM/MHEST

E-mail: tpopov@phys.uni-sofia.bg

Received 6 February 2011, in final form 28 April 2011
Published 9 March 2012
Online at stacks.iop.org/PSST/21/025004

Abstract
In this work, methods for using Langmuir probes (LPs) in magnetized plasmas are presented. The electron part of the current–voltage probe characteristics is used to obtain the plasma potential, the electron energy distribution function (EEDF), the electron temperature and the electron density. The application of LPs to EEDF evaluation in the presence of magnetic fields in the range 0.01–0.1 T is investigated and discussed based on kinetic theory in a non-local approach. Data for EEDFs in magnetic fields in the range 0.015–0.079 T are acquired using current–voltage characteristics measured in low pressure Ar and He dc gas discharges. It is also shown that the EEDFs are Maxwellian up to the energy of the first excited states of argon and helium. The values of the plasma potential, electron temperature and density are evaluated. Comparison of the results obtained with probes perpendicular and parallel to the magnetic field results in satisfactory agreement.

The results presented demonstrate that the procedures proposed allow one to acquire the main plasma parameters using the electron part of the current–voltage LP characteristics in magnetized plasmas.

(Some figures may appear in colour only in the online journal)

1. Introduction

Among the contact methods of plasma diagnostics, electric probes are the least expensive and remain the fastest and most reliable diagnostic tools allowing one to obtain the values of important plasma parameters; Langmuir probes (LPs) allow local measurements of the plasma potential, the charged particle density and the electron energy distribution function (EEDF), $f(\varepsilon)$ [1–5].

The probe technique is relatively simple when all the requirements of the 'classical' theory are satisfied, namely [6]:

(a) The plasma is isotropic within a scale much larger than the mean free path of the charged particles;
(b) the mean free paths of the electrons, λ, and ions, λ_i, are much larger than the probe radius, R, and the thickness of probe sheath, d;
(c) the probe holder does not disturb the plasma in the vicinity of the probe tip;
(d) there is neither generation nor recombination of charged particles, nor are there chemical reactions in the probe sheath or at the probe surface;
(e) the surface area of the reference probe is large enough to sustain all the current collected from the measuring probe without a noticeable potential drop;
(f) there are no fluctuations in the plasma characteristics;

(g) the probe surface is free of contamination, such as dielectric films.

Point (b) indicates that electrons originating from the undisturbed plasma and crossing the probe sheath reach the probe surface without any collision. This means that the probe operates at very low gas pressures or in a weak magnetic field when the electron mean free path λ or the Larmor radius R_L are larger than the probe radius R and the thickness of the sheath d [2–4]:

$$\lambda, R_L \gg R + d. \tag{1}$$

In the 'classical regime', probes operate in the absence of a magnetic field and at low gas pressures in the range 0.1–100 Pa. Then the electron probe current of the *IV* characteristic is expressed [2] by

$$I_e(U) = -\frac{2\pi eS}{m^2}\int_{eU}^{\infty}(W - eU)f(W)\,dW, \tag{2}$$

where e and m are the electron charge and mass, S is the probe area, $W = \frac{1}{2}mc^2 + eU$ is the total electron energy in the probe sheath and c is the electron velocity at the sheath edge. The probe is negatively biased by a potential U_p, U is the probe potential with respect to the plasma potential U_{pl}($U = U_p - U_{pl}$) and $f(\varepsilon)$ is the isotropic EEDF, normalized by

$$\frac{4\pi\sqrt{2}}{m^{3/2}}\int_0^{\infty} f(W)\sqrt{W}\,dW = \int_0^{\infty} f(\varepsilon)\sqrt{\varepsilon}\,d\varepsilon = n. \tag{3}$$

The EEDF can be determined using the Druyvesteyn formula [1]

$$f(\varepsilon) = \frac{2\sqrt{2m}}{e^3 S}\frac{d^2 I_e}{dU^2}. \tag{4}$$

In many different contemporary technologies, such as plasma chemistry, etching, plasma polymerization and thin layer dielectric deposition, relatively high gas pressures of 100–1000 Pa or a magnetic field in the range 0.01–0.1 T are required. In this case, due to the collisions in the probe sheath, the interpretation of the experimental data acquired in order to obtain the correct values of the plasma parameters becomes more complicated. This concerns EEDF probe measurements in a wide range of plasmas, from magnetron gas discharges to tokamak edge plasmas. Knowledge of the real EEDF is of great importance in understanding the underlying physics of processes occurring at the magnetized plasma, such as the formation of transport barriers, cross-field diffusion coefficients and plasma–substrate interactions. Although the electric probe method is as old as plasma physics itself, the potential of the method has not yet been fully exploited. New probe theories and designs constantly appear with the results summarized in numerous reviews and monographs [2–6]. In spite of this, incorrect applications of electric probes are commonly found in the literature. The errors mainly arise from a lack of awareness about the multitude of regimes of probe operation and the limits of validity of theories.

Swift [7] was the first to take into account the probe size and the effect of collisions in the probe sheath in evaluating the EEDF. He pointed out that the second derivative of the *IV* probe characteristic is distorted due to the depletion of electrons sinking on the probe surface at a finite R/λ ratio. Similar results on the applicability of the second derivative probe method were also obtained in [8, 9] through a more detailed analysis using kinetic theory in a non-local approach. In [10] the authors discussed an improved way of obtaining the EEDF at intermediate gas pressures (in the range 100–1000 Pa). In [9] it was shown that at high gas pressures (above 1000 Pa) the EEDF is represented by the first derivative instead of the second derivative of the electron probe current. The evaluation of the EEDF in a strongly magnetized plasma (magnetic field B in the range of 1–5 T) was discussed in [11], where the first derivative probe method was successfully applied to probe investigations of a tokamak edge plasma.

In this work, all requirements of the classical regime enumerated above with the exception of (b) are satisfied. We present probe measurements in argon and helium dc gas discharges in the presence of a magnetic field in the range 0.01–0.1 T with the aim of studying and, based on kinetic theory in a non-local approach, discussing the application of LPs in magnetized plasmas for evaluating the EEDF, $f(\varepsilon)$, the plasma potential, the electron temperature and the electron density.

2. Electron probe current measurements in magnetized plasmas

A kinetic theory for processing the electron probe current in the presence of a magnetic field was published in [8, 9]. The theory of magnetized plasmas was developed for LPs in a non-local approach when the electrons reach the probe in a diffusion regime. It was shown that the electron probe current is expressed by an extended equation

$$I_e(U) = -\frac{8\pi eS}{3m^2\gamma}\int_{eU}^{\infty}\frac{(W - eU)f(W)\,dW}{1 + ((W - eU)/W)\psi(W)} \tag{5}$$

The value of the geometric factor γ varies monotonically from 0.71 to 4/3: $\gamma = 4/3$ when $\lambda, R_L \gg R + d$ and $\gamma = 0.71$ when $\lambda, R_L \ll R + d$ [9].

The important parameter in equation (5) is the diffusion parameter $\psi = \psi(W)$. In the presence of a magnetic field B, ψ depends on the electron free path $\lambda(W)$ and Larmor radius $R_L(B, W)$, as well as on the shape, the size and the orientation of the probe with respect to the magnetic field.

Let us consider the limiting cases regarding the value of the diffusion parameter:

(1) When $\psi(W) \ll 1$ (low gas pressure and absence or very weak magnetic field), neglecting the second term $((W - eU)/W)\psi(W)$ in the denominator under the integral in equation (5) yields the classical expression for the electron probe current (1) and the EEDF can be determined using the Druyvesteyn formula (4). Although, as was shown by Swift [7], a drain of electrons to the probe is present at a finite R/λ ratio, the true value of $f(\varepsilon)$ at low probe potentials differs by less than 25% from that determined by the classical theory and the EEDF is well characterized by $I''(U)$.

(2) When $\psi(W) \sim 1$ (intermediate gas pressure and/or weak magnetic field) we have to use equation (5). Its second

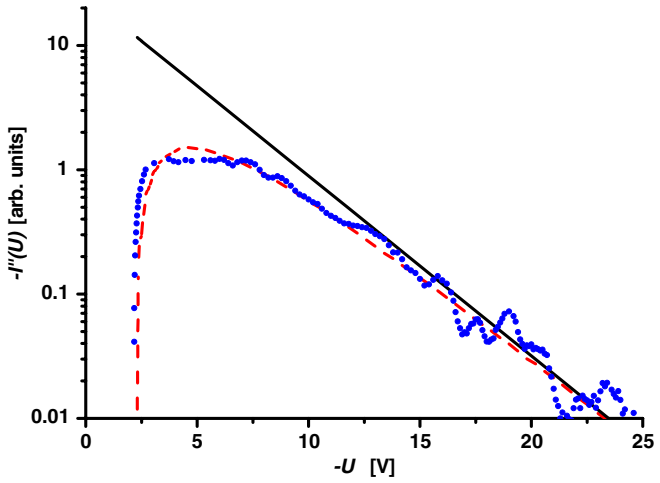

Figure 1. Comparison of the second derivative model curve (dashed line) for a Maxwellian EEDF ($T = 3$ eV) with the experimental curve (dots) at $\psi \sim 1$. The solid line presents the second derivative when $\psi \ll 1$.

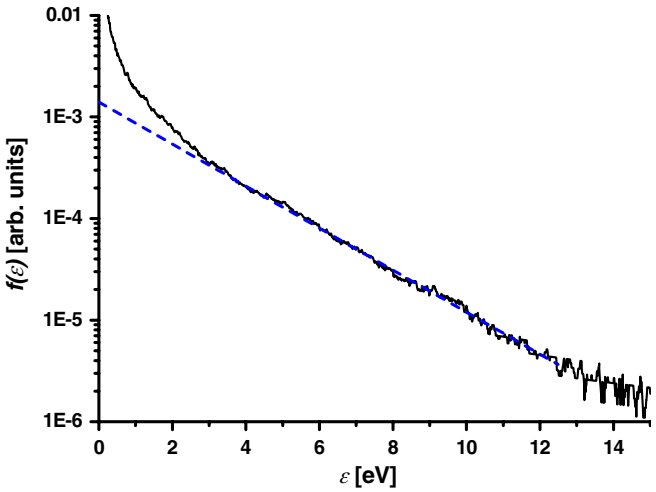

Figure 2. Comparison of the experimental (solid line) and model (dashed line) EEDF at electron temperature $T = 2.5$ eV and $\psi \gg 1$.

derivative yields the equation

$$I''(U) = Cf(eU) - C\int_{eU}^{\infty} K''(W,U)f(W)\,\mathrm{d}W, \qquad (6)$$

where

$$K''(W,U) = \frac{2\psi W^2}{[W(1+\psi) - \psi eU]^3}$$

and

$$C = \frac{8\pi e^3 S}{3m^2\gamma}.$$

The first term in equation (6) is the well-known Druyvesteyn formula. The second term describes the effect of plasma depletion caused by charged particles sinking on the probe surface.

Figure 1 presents model calculations at $\psi \sim 1$ for a Maxwellian EEDF with temperature $T = 3$ eV [10]. It is seen that the second derivative is not a good representation of the EEDF because $K''(W,U)$ decreases with the increase in U and of the energy of the electrons and only the high energy part of the EEDF at small R is well characterized by $I''(U)$. At small values of $U$and the electron energy, $K''(W,U) \approx 2\psi/(W(1+\psi)^3)$ increases indefinitely and $I''(U)$ decreases. In addition, the plasma potential U_{pl} does not coincide with the potential U^* at which the second derivative is zero $I''(U^*) = 0$, as is usually assumed. Consequently, an additional error will result if the concentration of the charged particles is obtained by integration over the second derivative.

In the case of a Maxwellian EEDF at $\psi(W) \sim 1$, a refined procedure based on obtaining the best fit between model calculations and experimental data was proposed and proved in [10]. The fitting parameters are the electron temperature, T, the electron density, n, and the plasma potential U_{pl}. The temperature is evaluated at high probe potentials where the second derivative is relatively weakly distorted. The next step is to calculate the second derivative following equation (6) using a Maxwellian EEDF normalized to 1. The results of the model calculations are fitted to the experimental curve using its maximum at low probe potentials. The plasma potential is evaluated by shifting the model curve along the U-axis, while the electron density is estimated by multiplying the model data by a coefficient to achieve the best fit.

(3) When $\psi(W) \gg 1$ (high gas pressure or magnetic field) the EEDF is represented by the first derivative instead of the second derivative as was shown in [9, 11, 12]:

$$I_{\mathrm{e}}'(U) = -\frac{8\pi e^2 S}{3m^2\gamma} \times \left(\frac{eU}{\psi} f(eU) + \int_{eU}^{\infty} \frac{Wf(W)\,\mathrm{d}W}{(1+\psi)[(1+\psi)W - \psi eU]}\right). \qquad (7)$$

In the case of high gas pressure plasmas or in magnetized plasmas, the contribution of the second term in equation (7) is usually assumed small and is therefore neglected.

The accurate evaluation of the EEDF requires that the value of the plasma potential, U_{pl}, be known. In [11] we proposed the following procedure: the electron temperature is evaluated from the slope in logarithmic scale of the first derivative of the experimental IV characteristic. Using this temperature, a model curve of the first derivative (derivative of equation (5)) is calculated. Then the best fit with the experimental first derivative provides the value of the plasma potential.

At $\psi \gg 1$ the EEDF is directly represented by the first derivative of the electron probe current:

$$f(\varepsilon) = \frac{3\sqrt{2m\gamma}}{2e^3 S}\frac{\psi}{U}\frac{\mathrm{d}I_{\mathrm{e}}}{\mathrm{d}U}. \qquad (8)$$

A comparison of the experimental and model EEDF at electron temperature $T = 2.5$ eV and $\psi(W) \gg 1$ is presented in figure 2. The discrepancy in the range of 0–2.5 eV is due to the mathematical approach rather than to physical phenomena [6].

It is obvious that to evaluate the EEDFs in cases (2) and (3), the values of the diffusion parameter must be known. The solution in the general case is presented in [8, 9].

The kinetic equation for the isotropic EEDF in the absence of a magnetic field is [8]

$$\nabla_r D(w)\nabla_r f(W,r) = 0, \tag{9}$$

where $D(w) = cD_r = c^2\lambda/3$. The boundary conditions are

$$f(r \to \infty, W) = f_\infty(W), \tag{10}$$

$$f(R, W > eU) = \gamma f_1(R, W). \tag{11}$$

Here the anisotropic part of EEDF is $f_1(r, W) = -\lambda\nabla_r f(r, W) = -\lambda\partial f/\partial r$.

To generalize the problem, the probe is considered as an ellipsoid of revolution [9] with dimensions R and $b = L/2$ (L being the probe length). Since the probe surface is equipotential, the diffusion equation (9) depends on the elliptical coordinate σ, determined as

$$\frac{x^2+y^2}{R^2(\sigma^2 \pm 1)} + \frac{z^2}{R^2\sigma^2} = 1. \tag{12}$$

At the probe surface $\sigma = \sigma_0 = b/\beta$, $\beta = (|b^2 - R^2|)^{1/2}$ and the '+' and '−' signs refer to oblate ($b < R$) and prolate ($b > R$) ellipsoids, respectively.

The boundary condition (10) remains the same, but the condition (11) can be written as

$$\sigma = \sigma_0 \qquad \frac{\lambda}{S}2\pi\beta(\sigma^2-1)\frac{\partial}{\partial\sigma}f = \frac{1}{\gamma}f. \tag{13}$$

The solution of equation (9) with boundary conditions (10) and (13) yields the extended equation for electron probe current (5) with diffusion parameter:

$$\psi(W) = \frac{S}{4\pi\beta\gamma\lambda(W)}\int_{\sigma_0}^{\infty}\frac{D(W)d\sigma}{(\sigma^2 \mp 1)D(W - e\phi(\sigma))}. \tag{14}$$

Here $D(W)$ is the diffusion coefficient in bulk plasma and $D(W - e\phi(\sigma))$ is that in the probe sheath ($\phi(\sigma)$ being the potential variation introduced by the probe). Assuming a constant coefficient of diffusion, for a thin sheath we have

$$\psi(\varepsilon) = \frac{S}{8\pi\beta\lambda(\varepsilon)\gamma}\ln\left(\frac{\sigma_0+1}{\sigma_0-1}\right) \qquad b > R,$$
$$\psi(\varepsilon) = \frac{S}{8\pi\beta\lambda(\varepsilon)\gamma}(\pi - 2\arctan\sigma_0) \qquad b < R. \tag{15}$$

In the presence of a magnetic field, the coefficient of diffusion $D(W)$ in equation (9) becomes a tensor with two components:

$$D_\parallel(w) = c^2\lambda/3 \quad \text{and} \quad D_\perp(w) = D_\parallel(w)/\rho^2,$$
$$\text{where } \rho = \left[1 + \left(\frac{\lambda}{R_L}\right)^2\right]^{1/2}.$$

In this case, the kinetic equation for the EEDF has the form of the anisotropic diffusion equation:

$$D_\perp(w)\Delta_r f + D_\parallel(w)\Delta_z f = 0. \tag{16}$$

As we mentioned above, the solution for $\psi(W)$ depends on the probe orientation with respect to the magnetic field. Let us consider a probe placed along the magnetic field. Changing the scale $z \to z'/\rho$ we can reduce the problem to the one solved above so that for the diffusion parameter we have

$$\psi_\parallel(W) = \frac{S\rho}{8\pi\beta_\parallel^M\lambda(W)\gamma}\ln\left(\frac{\sigma_\parallel^M+1}{\sigma_\parallel^M-1}\right) \qquad b' > R, \tag{17a}$$

$$\psi_\parallel(W) = \frac{S\rho}{8\pi\beta_\parallel^M\lambda(W)\gamma}(\pi - 2\arctan\sigma_\parallel^M) \qquad b' < R, \tag{17b}$$

where $\beta_\parallel^M = (|R^2 - b'^2|)^{1/2}$, $b' = b/\rho$, $\sigma_\parallel^M = b'/(|R^2 - b'^2|)^2 = b'/\beta_\parallel^M$.

For a probe placed across the magnetic field using this approach with general ellipsoidal coordinates, the diffusion parameter is found to be [9, 13]

$$\psi_\perp(W) = \frac{S\rho}{4\pi\beta_\perp^M\lambda(W)\gamma}F(\phi/\alpha), \tag{18}$$

where $F(\phi/\alpha)$ is an incomplete elliptical integral of the first kind [14] and

$$\beta_\perp^M = (|R'^2 - b^2|)^{1/2} \quad R' = \frac{R}{\rho} \qquad \cos(\phi) = \frac{R}{b}$$
$$\cos(\alpha) = \frac{(R^2 - R'^2)}{\beta_\perp^M}.$$

The results presented are important, but for practical use they need to be simplified bearing in mind the actual plasma conditions. Let us consider a cylindrical probe with radius $R = 1 \times 10^{-4}$ m and length $L = 5 \times 10^{-3}$ m. For an argon gas discharge at gas pressure $p \sim 1$ Pa and magnetic fields in the range $B = 0.01$–0.1 T with the probe located along the magnetic field we have

$$\lambda \sim 1\,\text{m} \qquad R_L \sim 10^{-5}\,\text{m}, \qquad \rho \sim 10^5, \qquad \sigma_\parallel^M \sim 10^{-3}.$$

Then $R \gg b'$; $\pi \gg 2\arctan 10^{-3}$ and since

$$\rho = \left[1 + \left(\frac{\lambda}{R_L}\right)^2\right]^{1/2} \approx \frac{\lambda(W)}{R_L(B,W)},$$

using equation (17*b*) we arrive at

$$\psi_\parallel(W) = \frac{b\rho}{2\lambda(W)\gamma}\pi = \frac{\pi L}{4\gamma R_L(B,W)} = \frac{\psi_0^\parallel}{\sqrt{W}}. \tag{19}$$

Here $\psi_0^\parallel$ is constant with respect to the energy part of the diffusion parameter.

When the probe is placed across the magnetic field, using equation (18) we obtain

$$\psi_\perp(W) = \frac{R}{\gamma R_L(B,W)}F(\phi/\alpha). \tag{20}$$

Demidov *et al* [15, 16] used a different approach for the diffusion parameter when the probe is placed across the magnetic field:

$$\psi_\perp(W) = \frac{R}{\gamma R_L(B,W)}\ln\left(\frac{\pi L}{4R}\right). \tag{21}$$

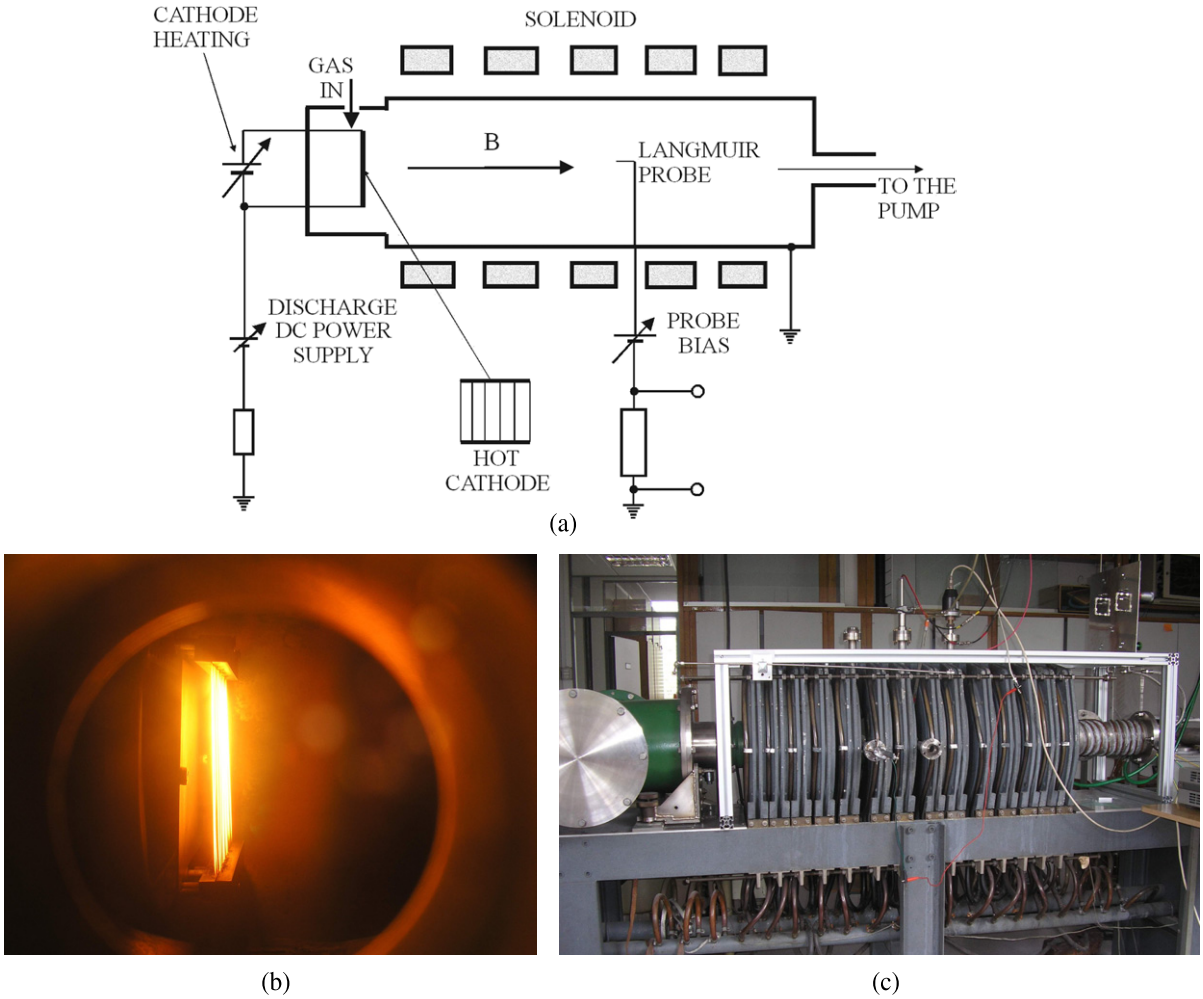

Figure 3. Schematic representation of the experimental set-up (*a*) and photographs of the emissive cathode (*b*) and the solenoid (*c*).

At large values of the parameter ρ equation (21) yields values for the diffusion parameter 6–8% lower than the one obtained by equation (20), but this difference in practice does not affect the general results for the plasma parameters acquired. For more complicated non-homogeneous plasmas (flowing, turbulent, chemically active, etc) there are indications that the probe length L in equation (21) must be increased up to the characteristic length of the inhomogeneity L', e.g., the characteristic length of turbulence [11]. The problem is still under investigation and is beyond the scope of this work.

In both cases, we also may use the diffusion parameter in the form

$$\psi_{\perp}(W) = \frac{\psi_0^{\perp}}{\sqrt{W}}.$$

3. Experimental results and discussion

The plasma was produced in a stainless-steel discharge tube with length 1.5 m and diameter 0.17 m (figure 3(*a*)) with a hot filament cathode (figure 3(*b*)). The wall of the discharge tube was grounded. A negative potential of −35 V was applied to the cathode while the gas discharge current was kept constant at 2 A. An axial magnetic field B was created by a solenoid (figure 3(*c*)) and was varied from 0.015 T to 0.079 T. The working gases were argon and helium at pressure $p = 0.8$ Pa.

The cylindrical LP with $R = 1 \times 10^{-4}$ m and length $L = 5 \times 10^{-3}$ m was placed axially and radially at the centre of the discharge tube. The probe surface was cleaned by ion bombardment by applying a large negative potential before measuring the IV probe characteristics. The measurements were performed with the probe oriented in parallel and perpendicular to the magnetic field. The derivatives were calculated numerically. The results of the measurements of the plasma parameters at different values of the magnetic field are presented in table 1.

The accuracy of the electron temperature evaluation was 10%. Taking into account the uncertainties in all the values measured, the uncertainty in the electron density evaluation did not exceed 25%. The accuracy of the plasma potential evaluation was 20%. The discrepancies between the plasma potential values measured by the perpendicular and the parallel probe in the range of magnetic fields from 0.055 T to 0.079 T can be explained by the radial averaging in the measurements by a perpendicular probe, since the parallel probe was oriented along the magnetic field lines.

In evaluating the uncertainties, additional factors (according to the classical regime requirements with the

Table 1. Experimental results of the plasma parameters at different values of the magnetic field and different orientations of the probe.

		Perpendicular probe							Parallel probe						
		Second derivative			First derivative				Second derivative			First derivative			
B (T)	ψ_0	T (eV)	$n \times 10^{18}$ (m^{-3})	U_{pl} (V)	T (eV)	$n \times 10^{18}$ (m^{-3})	U_{pl} (V)	ψ_0	T (eV)	$n \times 10^{18}$ (m^{-3})	U_{pl} (V)	T (eV)	$n \times 10^{18}$ (m^{-3})	U_{pl} (V)	
Ar															
0.015	**1.2**	3.2	0.5	3.2	—	—	—	**13**	3.2	1.1	6.2	2.4	1	6.2	
0.025	**2**	2.9	1.5	4	—	—	—	**21**	2.9	2.4	5.9	2.5	2.1	5.3	
0.035	**2.9**	2.3	4.0	4.6	—	—	—	**30**	2.3	4.5	5.2	2.1	4.1	5	
0.045	**3.7**	2.2	4.8	4.1	2.2	4.3	5	**38**	2	6	4.5	2	4.8	4	
0.055	**4.6**	2.1	6.0	3.6	2.2	6.0	3.8	**48**	—	—	—	1.8	6.4	2.5	
0.065	**5.4**	2.1	6.4	2.7	2.1	6.4	3.2	**55**	—	—	—	1.8	6.4	1.7	
0.079	**6.5**	2.3	7.5	2	2.3	7.4	2	**67**	—	—	—	1.7	7.6	0.2	
He															
0.015	**1.2**	2.3	0.5	0.5	—	—	—	**13**	2.3	0.8	0.9	2.1	0.6	1	
0.025	**2**	2.3	0.9	−2.7	—	—	—	**21**	2.3	1.1	−2.3	2.1	1.1	−3	
0.035	**2.8**	2.2	0.8	−4.4	—	—	—	**30**	2.2	1	−4	2.2	0.9	−5	

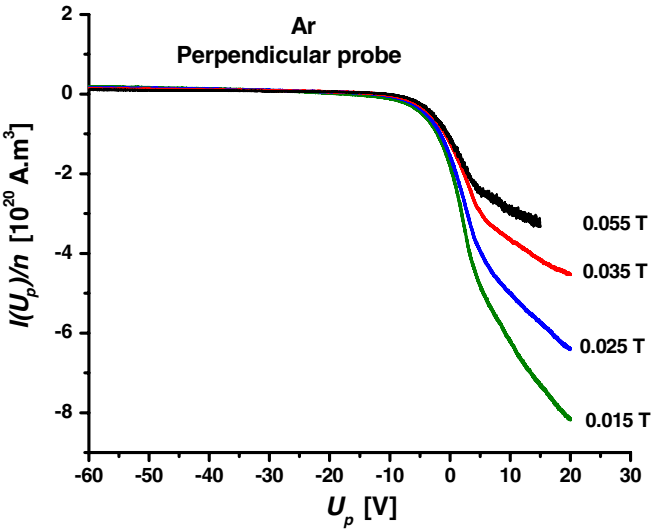

Figure 4. Electron probe current normalized to the electron density measured by a probe oriented perpendicularly to the magnetic field.

exception of (b)) affecting the accuracy of the data measured were taken into account [10].

It is seen that as the magnetic field is increased, the electron density increases, which can be explained by the decrease in the cross-field diffusion of the electrons to the wall of the discharge tube. The influence of the magnetic field on the *IV* probe characteristics measured is illustrated in figure 4, where the probe current is normalized to the electron density.

An example of the extended second derivative probe method application when the value of the diffusion parameter is relatively small is shown in figure 5. In an argon gas discharge and in the presence of a magnetic field of 0.025 T, the EEDF is Maxwellian with a temperature of 2.9 eV. The instrumental function of the differentiation technique is triangular with a half-width equal to the step change in the probe bias [6, 10, 17]. To take into account the instrumental function influence when the experimental and model curves were compared, both of them were smoothed and differentiated in the same way.

As the value of the diffusion parameter increases, both techniques, namely, the extended second derivative technique and the first derivative technique, can be employed (figures 6(*a*) and (*b*))

In figure 7, a comparison is presented of evaluating the EEDF by a perpendicular and a parallel probe for the same conditions at 0.025 T. The results obtained are in satisfactory agreement.

We must note that in our case the second derivative probe method can be used up to values of $\psi_0 \sim 30$–35, when the level of the signal-noise ratio is still acceptable.

When using the first derivative probe method at relatively low values of ψ_0, as in the case of the perpendicular probe we have to use equation (7) for evaluating the EEDF. At relatively high values of the diffusion parameter, we must check for the contribution of the second term in equation (7). Concerning the results presented in figure 6(*b*), a comparison between the experimental first derivative and the model calculations results is presented in figure 8:

One can see that the contribution of the second term is within the experimental error. Then, bearing in mind equation (19), to evaluate the EEDF we can use the expression for a probe oriented in parallel to the magnetic field:

$$f(\varepsilon) = -\frac{3\pi\sqrt{2m}L}{8e^3 S R_L(B,\varepsilon)U}\frac{\mathrm{d}I}{\mathrm{d}U}. \qquad (22)$$

The comparison of the results obtained with the extended second derivative and the first derivative probe methods show satisfactory agreement. When comparing the methods, we should emphasize that the first derivative probe method directly yields the EEDF not only in the Maxwellian case but also when the energy distribution of the electrons deviate from the Maxwellian. The application of the extended second derivative probe method when the EEDF is non-Maxwellian is more complicated: mathematically speaking, to deduce the EEDF from probe measurements under collisional conditions requires that two coupled inverse problems be solved, since the distortion of the second derivative includes an integral over the unknown EEDF and the data are convoluted by the instrumental function [10].

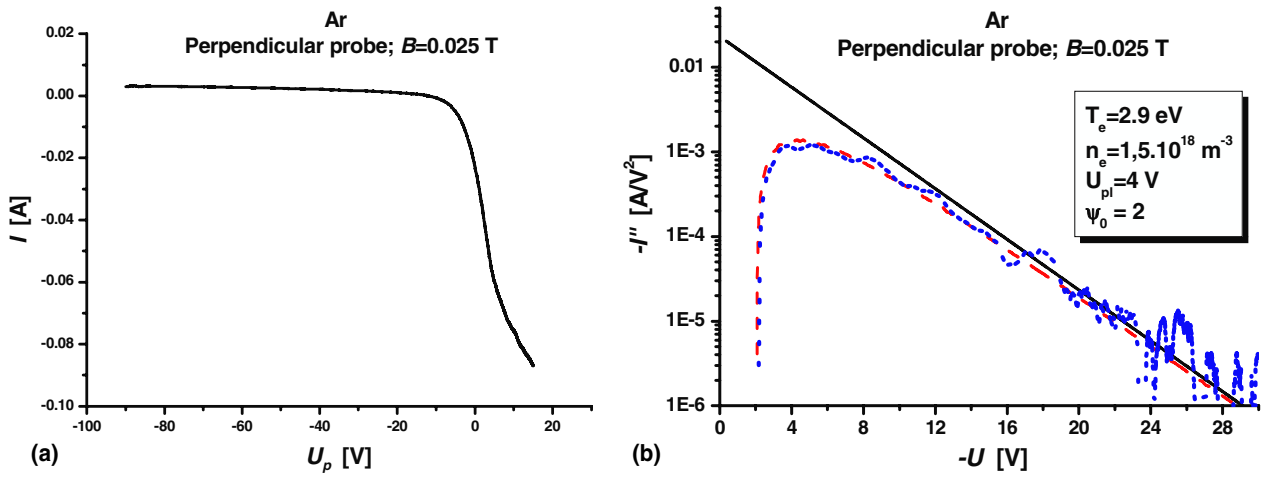

Figure 5. (*a*) *IV* probe characteristic measured in an argon gas discharge in the presence of a magnetic field of 0.025 T. (b) Comparison of the experimental second derivative of the electron probe current (dots) with the model calculations (dashed line) in the case of a Maxwellian EEDF (solid line).

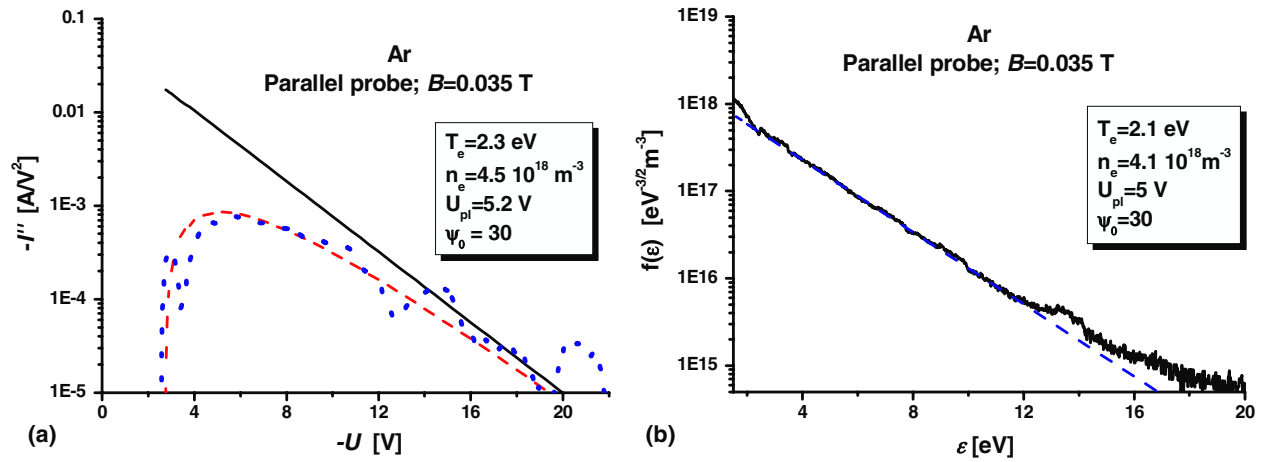

Figure 6. (*a*) Comparison of the experimental second derivative of the electron probe current (dots) with the model calculations (dashed line) in the case of a Maxwellian EEDF (solid line). (*b*) Evaluated EEDF (solid line) in argon gas discharge in the presence of a magnetic field of 0.035 T and model Maxwellian EEDF (dashed line) at an electron temperature of 2.1 eV.

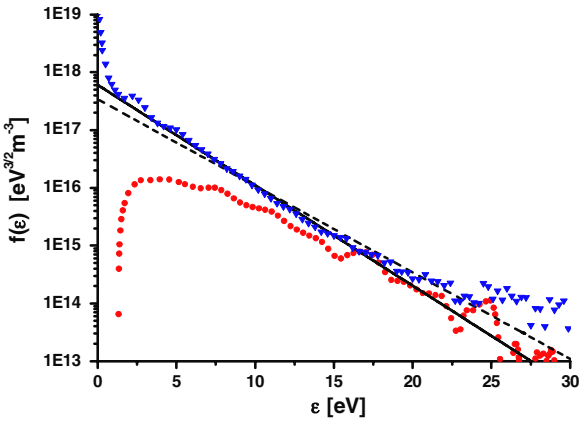

Figure 7. Evaluated EEDF (triangles) measured with a parallel probe in an argon gas discharge in the presence of a magnetic field of 0.025 T and model Maxwellian EEDF (solid line) at electron temperature of 2.5 eV. Evaluated EEDF (gashed line) by perpendicular probe using second derivative of the electron probe current (dots) at an electron temperature 2.9 eV.

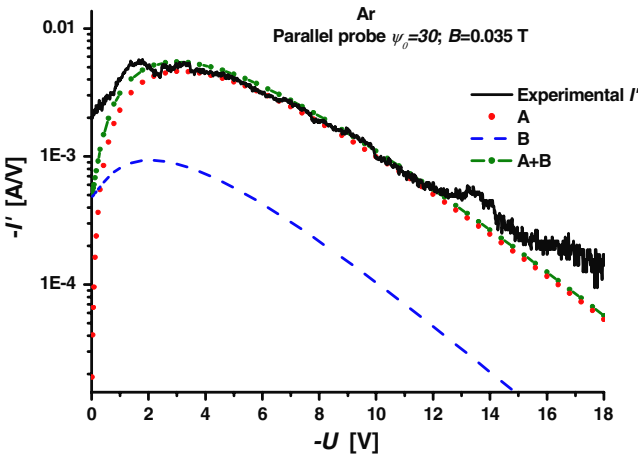

Figure 8. The experimental first derivative is presented by a solid line. The first term of equation (7) is $A = -(8\pi e^2 S/3m^2\gamma)(eU/\psi) f(eU)$. $B = -(8\pi e^2 S/3m^2\gamma) \int_{eU}^{\infty} (Wf(W)\,\mathrm{d}W/((1+\psi)[(1+\psi)W - \psi eU]))$ is the second term. A+B corresponds to equation (7).

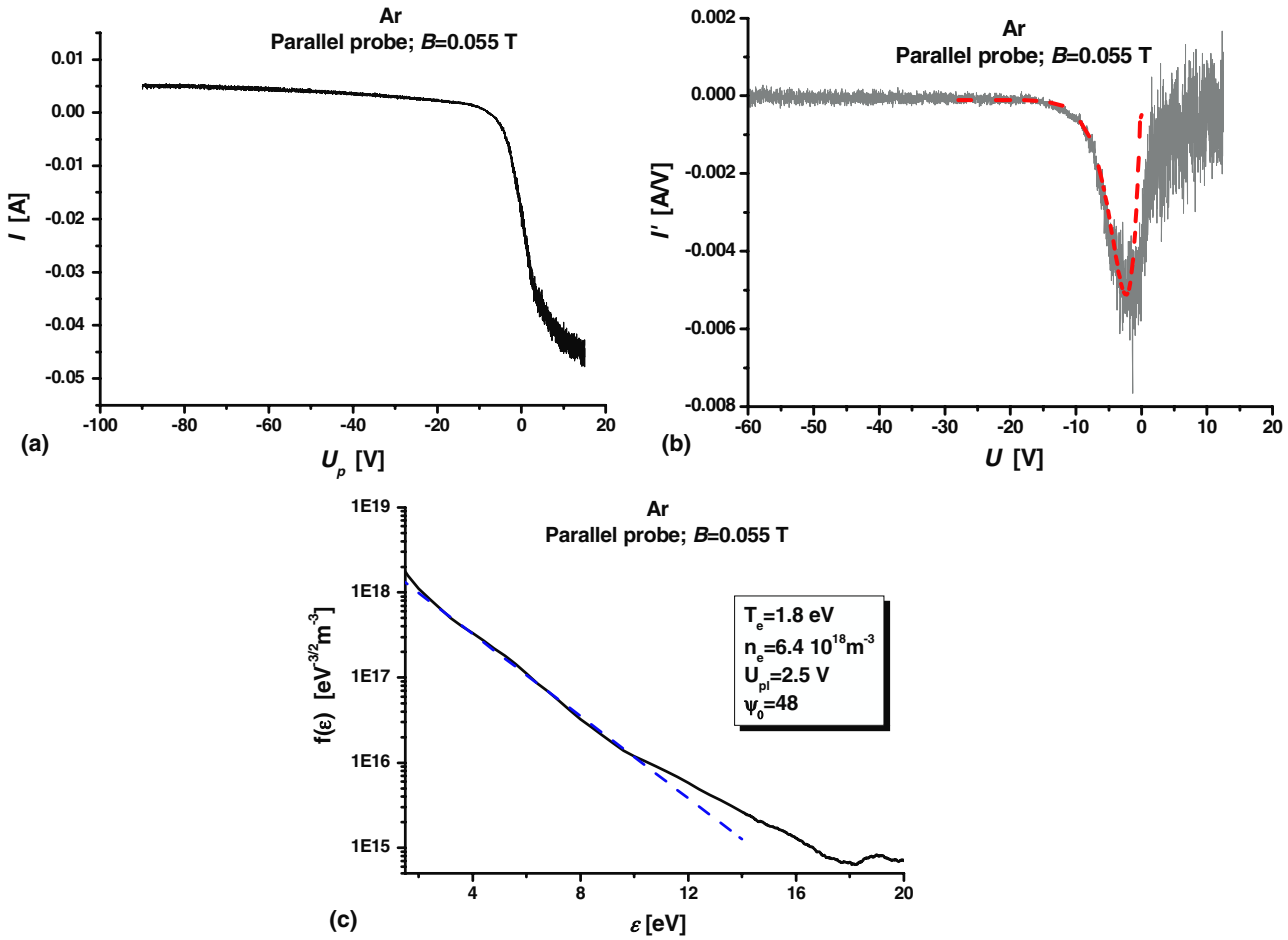

Figure 9. (*a*) *IV* probe characteristic measured in an argon gas discharge in the presence of a magnetic field of 0.055 T. (*b*) Comparison between the experimental first derivative (solid line) and model curve (dashed line) for obtaining the plasma potential. (*c*) Evaluated EEDF (solid line) in an argon gas discharge in the presence of a magnetic field of 0.055 T and model Maxwellian EEDF (dashed line) at an electron temperature of 1.8 eV.

Expression (22) is used to evaluate the EEDF at a magnetic field $B = 0.055$ T in an argon gas discharge (figure 9). Figure 9(*a*) presents the experimental *IV* probe characteristic measured with the probe parallel to the magnetic field. Figure 9(*b*) is a comparison between the experimental first derivative and the model curve in view of evaluating the plasma potential [11]. To coincide with the model curve (where the plasma potential is set at zero) the experimental curve is shifted by 2.5 V, which is the value of the plasma potential. Because of the influence of the magnetic field, the minimum of the curves is shifted away from the plasma potential at a distance equal to the electron temperature value expressed in volts. The discrepancy between the model curve and the experimental curve behaviour after the minimum is due to the fact that the probe current does not saturate after the probe bias reaches the plasma potential. A more or less pronounced change in the experimental curve slope can be seen near the plasma potential.

Figure 9(*c*) shows the evaluated EEDF (solid line) in an argon gas discharge in the presence of a magnetic field of 0.055 T. The EEDF is generally Maxwellian, although after the energy of the first excited state of argon (11.55 eV) the influence of a group of faster electrons can be seen (figure 10). The effect becomes more pronounced as the value of the magnetic field applied is raised. To clarify this, additional experiments must be performed at different gas pressures in combination with optical measurements of the metastable states population [18, 19].

While the Ar gas discharge was very stable without significant fluctuations of the plasma potential and noises within the entire interval of magnetic field variation, the value of the noise amplitude increased rapidly in He discharges at magnetic fields above 0.035 T; thus, the probe measurements were performed up to this value of the applied magnetic field.

An example of the EEDF measured in a He gas discharge with a probe oriented in parallel to a magnetic field of 0.015 T is presented in figure 11.

4. Conclusion

In this work, methods for using LPs in magnetized plasmas are presented. The electron part of the current–voltage probe characteristics was used to obtain the plasma potential, the EEDF, the electron temperature and the electron density:

- The application of LPs to EEDF evaluation in the presence of magnetic fields in the range 0.01–0.1 T was investigated and discussed based on kinetic theory in a non-local

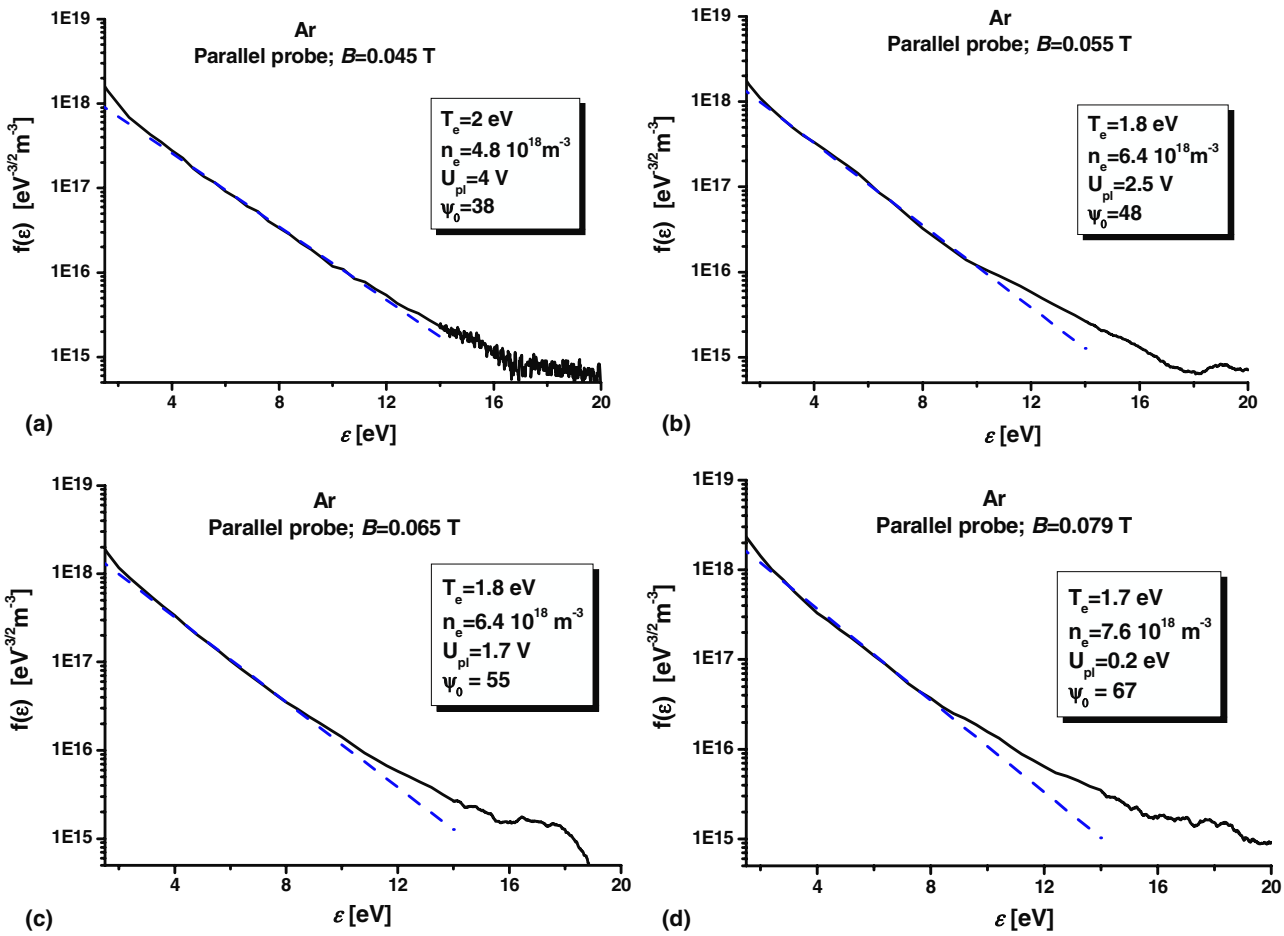

Figure 10. Comparison of the EEDF (solid lines) obtained by measurements with a probe in parallel to magnetic fields of different values. The model Maxwellian EEDF is presented by dashed lines.

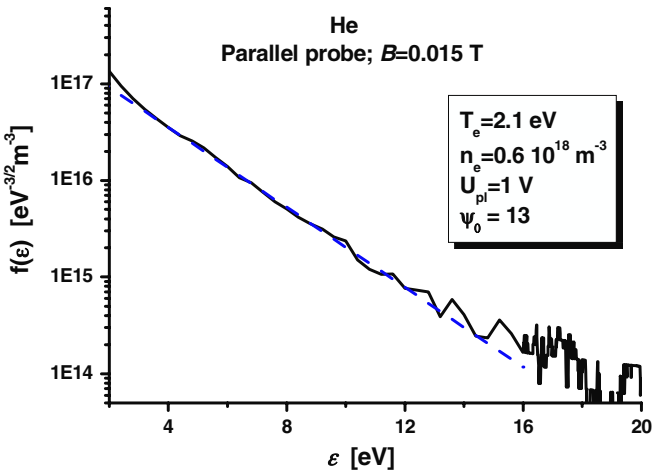

Figure 11. EEDF measured in a He gas discharge with a probe oriented parallel to the magnetic field of 0.015 T.

approach. The diffusion parameter in an extended formula of the electron probe current was estimated for cylindrical probes oriented perpendicular and parallel to the magnetic field lines.

- Data for EEDFs in magnetic fields in the range 0.015–0.079 T were acquired using current–voltage characteristics measured in low pressure Ar and He dc gas discharges. It was shown that at diffusion parameter values $\psi \sim 1$, the extended second derivative method must be used, while at $\psi \gg 1$, the first derivative of the electron probe current yields a good representation of the EEDF. At intermediate values of the diffusion parameter, the two methods yield comparable results.
- It was also shown that the EEDFs are Maxwellian up to the energy of the first excited states of argon and helium. The values of the plasma potential, electron temperature and density were evaluated. Comparison of the results obtained with probes perpendicular and parallel to the magnetic field resulted in satisfactory agreement.

The results presented demonstrate that the procedures proposed allow one to acquire the main plasma parameters using the electron part of the current–voltage LP characteristics in magnetized plasmas.

Acknowledgments

This work, supported by the European Communities under the Contract of Association between EURATOM and INRNE.BG (task P4 of Work Plan 2010) and EURATOM and MHEST, was carried out within the framework of the European Fusion

Development Agreement. The content of the publication is the sole responsibility of its authors and it does not necessarily represent the views of the Commission or its services. The visit of TsvKP and PI to Ljubljana was also partially supported by the CEEPUS II, network AT-0063-01-0506 2010 mobility program.

References

[1] Druyvesteyn M J 1930 *Z. Phys.* **64** 781–98
[2] Kagan Y M and Perel V I 1964 *Sov. Phys.—Usp.* **6** 767
[3] Chen F F 1965 *Electric Probes in Plasma Diagnostic Techniques* ed R H Huddlestone and S L Leonard (New York: Academic) chapter 4, pp 113–200
[4] Swift J D and Schwar M J R 1969 *Electrical Probes for Plasma Diagnostic.* (New York: Elsevier)
[5] Hershkowitz N 1989 How Langmuir probes work *Plasma Diagnostics* vol 1, ed O Auciello and D L Flamm (Boston, MA: Academic) chapter 3
[6] Demidov V I, Kolokolov N B and Kudriavtsev A A 1996 *Probe Methods for Low-TemperaturePlasma Investigations* (Moscow: Energoatomizdat) (in Russian)
[7] Swift J D 1962 *Proc. Phys. Soc.* **79** 697–701
[8] Golubovsky Yu B, Zakharova V M, Pasunkin V I and Tsendin L D 1981 *Sov. J. Plasma Phys.* **7** 340
[9] Arslanbekov R R, Khromov N A and Kudryavtsev A A 1994 *Plasma Sources Sci. Technol.* **3** 528
[10] Popov Tsv K, Dimitrova M, Dias F M, Tsaneva V N, Stelmashenko N A, Blamire M G and Barber Z H 2006 *J. Phys. Conf. Series* **44** 60–9
[11] Popov Tsv K, Ivanova P I, Stockel J and Dejarnac R 2009 *Plasma Phys. Control. Fusion* **51** 065014
[12] Demidov V I, Ratynskaia S V and Rypdal K 2002 *Rev Sci Instrum.* **73** 3409–39
[13] Mal'kov M A 1991 *High Temp.* **29** 429
[14] Abramowitz M and Stegun I A 1972 *Handbook of Mathematical Functions* (New York: Dover)
[15] Demidov V I, Ratynskaia S V, Armstrong J and Rypdal K 1999 *Phys. Plasmas* **6** 350–8
[16] Demidov V I, Ratynskaia S V and Rypdal K 2001 *Contrib. Plasma Phys.* **41** 443–8
[17] Blagoev A B, Demidov V I, Kolokolov N B and Toronov O G 1981 *Sov. Phys. Tech. Phys.* **26** 1179–83
[18] Blagoev A B and Popov T 1979 *Phys. Lett.* A **70** 416
[19] Blagoev A, Mishonov T and Popov T 1984 *J Phys. B*: *At. Mol. Phys.* **17** 435